RESEARCH ARTICLE

WILEY

Altered resting-state functional network connectivity in profound sensorineural hearing loss infants within an early sensitive period: A group ICA study

Shanshan Wang[1] | Boyu Chen[1] | Yalian Yu[2] | Huaguang Yang[3] | Wenzhuo Cui[1] | Guoguang Fan[1] | Jian Li[1]

[1]Department of Radiology, The First Hospital, China Medical University, Shenyang, Liaoning, China

[2]Department of Otorhinolaryngology, The First Hospital, China Medical University, Shenyang, Liaoning, China

[3]Department of Radiology, Renmin Hospital, Wuhan University, Wuhan, China

Correspondence
Guoguang Fan and Jian Li, Department of Radiology, The First Hospital, China Medical University, #155, Nanjing North St., Heping Dist., Shenyang, Liaoning 110001, China.
Email: fanguog@sina.com (G. F.) and xikuang512@163.com (J. L.)

Abstract

Data from both animal models and deaf children provide evidence for that the maturation of auditory cortex has a sensitive period during the first 2–4 years of life. During this period, the auditory stimulation can affect the development of cortical function to the greatest extent. Thus far, little is known about the brain development trajectory after early auditory deprivation within this period. In this study, independent component analysis (ICA) technique was used to detect the characteristics of brain network development in children with bilateral profound sensorineural hearing loss (SNHL) before 3 years old. Seven resting-state networks (RSN) were identified in 50 SNHL and 36 healthy controls using ICA method, and further their intra-and inter-network functional connectivity (FC) were compared between two groups. Compared with the control group, SNHL group showed decreased FC within default mode network, while enhanced FC within auditory network (AUN) and salience network. No significant changes in FC were found in the visual network (VN) and sensorimotor network (SMN). Furthermore, the inter-network FC between SMN and AUN, frontal network and AUN, SMN and VN, frontal network and VN were significantly increased in SNHL group. The results implicate that the loss and the compensatory reorganization of brain network FC coexist in SNHL infants. It provides a network basis for understanding the brain development trajectory after hearing loss within early sensitive period.

KEYWORDS
functional connectivity, independent component analysis, resting-state network, sensitive period, sensorineural hearing loss

1 | INTRODUCTION

The prevalence of permanent childhood hearing loss is 1.2–1.7 cases per 1,000 live births. In developing countries, the prevalence is greater (Kral & O'Donoghue, 2010). Sensorineural hearing loss (SNHL) is mainly due to alterations in the inner ear, vestibulocochlear nerve (cranial nerve VIII) or central processing centers of the brain (Chen & Oghalai, 2016). The effects of early onset hearing loss on communication development, as well as educational and social development, are well documented (Huang et al., 2015; Liu et al., 2015; Tarabichi

et al., 2017). Appropriate early intervention, especially cochlear implants (CI), is an effective way of restoring hearing in children with congenital profound SNHL (Kral & O'Donoghue, 2010).

The explosive growth of brain structure and function in infancy is unparalleled by any other postnatal developmental period. Researchers studying the auditory cortex have reported that peak synaptic density is attained at 2–4 years of age in children with typical hearing (Kral & O'Donoghue, 2010). Furthermore, electroencephalographic studies on implanted children have also established the existence of a "sensitive period" for CI within the first 3.5–4.0 years after birth (Kral & Sharma, 2012; Sharma & Campbell, 2011; Sharma, Campbell, & Cardon, 2015). Therefore, a better understanding of the brain specific functional mechanisms within this early sensitive period is urgently needed to pave the way for early identification and interventions for profound SNHL patients.

Resting-state functional MRI (rs-fMRI) measures the low-frequency component of the blood oxygen level dependent (BOLD) signal in the absence of an explicit task. Attributed to its intrinsic characteristic of minimum/no demands for subject participation, rs-fMRI is recognized as an ideal tool for investigating the neurodevelopment in infancy (Mongerson, Jennings, Borsook, Becerra, & Bajic, 2017; Smyser & Neil, 2015). Functional connectivity (FC) analyses through rs-fMRI might provide underlying evidence to reflect the intrinsic interactions among discrete neuroanatomical regions (De, Beckmann, De, Matthews, & Smith, 2006; Fox & Raichle, 2007). Studies in subjects with hearing loss have shown altered FC not only in regions directly associated with auditory processing, but also in visual, sensorimotor and higher-order structures (Husain, Carpenter-Thompson, & Schmidt, 2014; Li et al., 2013; Propst & Greinwald, 2010; Shi et al., 2016; Wang et al., 2014; Xia et al., 2017). For example, the primary auditory cortex (A1) was found less connected with the motor cortex, whereas the visual cortex showed strengthened connectivity with motor and speech cortices in congenitally deaf children compared with the controls (Shi et al., 2016). Weaker FC of middle superior temporal sulcus and anterior superior temporal sulcus has been found both in congenitally deaf and acquired deaf adult patients (Li et al., 2013). Moreover, our previous study found increased FC between left/right primary auditory cortex seeds and insula, superior temporal gyrus in profound SNHL children before 3 years of age (Wang et al., 2019). The decreases and increases in FC presented in these results were suggesting that both functional loss and compensatory plasticity occur after auditory deprivation. Recently, investigations of the intrinsic FC of the human brain have demonstrated that the brain is organized into multiple resting-state networks (RSNs). These RSNs are characterized by spatially coherent, spontaneous fluctuations in the BOLD signal and are known to mirror functional networks activated during task-oriented behaviors (Biswal, Van Kylen, & Hyde, 1997; Cordes et al., 2001; Fox & Raichle, 2007). A variety of RSNs has been identified including visual, somatosensory, and auditory networks, as well as higher integrative networks, such as language, attention, salience networks, and the default mode network (DMN) (Smith et al., 2009; Zhang & Raichle, 2010). In adult patients with unilateral hearing loss (UHL), brain function changes and/or FC

changes were found in regions associated to the auditory, visual, sensorimotor, default mode, execution, language and attention networks (Liu et al., 2015; Wang et al., 2014; Yang et al., 2014), and the changes in DMN might affect cognitive abilities in UHL patients (Zhang et al., 2015; Zhang et al., 2016). Studies on children (7–17 years) with UHL demonstrated multiple FC changes between brain networks involved with auditory, sensorimotor, executive function, cognition, and language comprehension (Jung, Colletta, Coalson, Schlaggar, & Lieu, 2017; Tibbetts et al., 2011). Results of these studies suggested multimodal interactions both within and between RSNs after hearing damage. However, such studies typically only focus on several predefined ROIs and thus do not yield an optimal representation of the RSN patterns across the whole brain.

Independent component analysis (ICA) is a primarily data-driven method (Beckmann, Deluca, Devlin, & Smith, 2005; Smith et al., 2009), which has been found to be able to capture the complex nature of fMRI time courses as well as to produce consistent spatial (statistically distinct) components (Calhoun & Adali, 2006; Turner & Twieg, 2005). The benefit of the ICA approach is that all significantly weighted voxels within an independent component are highly correlated, and can be available for identifying multiple whole-brain RSNs and further for quantifying intra and internetwork FC among RSNs (-Jafri, Pearlson, Stevens, & Calhoun, 2008). Using ICA, Luan et al. (2019) found that long-term SNHL involves notable dysconnectivity of multiple RSNs. Compared lightly anesthetized hearing and neonatally deafened cats, Stolzberg and their colleagues found FC amplitude differences included regions involved in auditory-related networks and visual, cingulate, somatosensory networks using ICA (Stolzberg, Butler, & Lomber, 2018). It indicates that both compensatory plasticity and a general loss of function likely coexist between various networks in the early deaf brain. However, reports of FC changes from ICA are limited in young children especially in SNHL infants within early sensitive period.

In the current study, we performed ICA method of rs-fMRI data to assess FC patterns both within and between RSNs in bilateral profound SNHL patients before 3 years old. Based on the background, we hypothesized that SNHL patients and controls would differ significantly on intra-network FC measures of both sensory-related and cognitive-related RSNs. In addition, we attempted to detect whether there are any changes in the inter-network FC between RSNs.

2 | METHODS

2.1 | Participants

This study is comprised of 95 subjects: 56 patients (30 females; mean age 17.89 ± 7.81 months) with congenital bilateral profound SNHL and 39 healthy controls (HC) (20 females; mean age 17.59 ± 6.95 months). The data for the present study were part of our previous study (Wang et al., 2019), with some new subjects added. All SNHL participants failed the newborn hearing screening examinations. As a confirmatory test, the auditory brainstem response (ABR) was

measured at 42 days. All the patients with ABR results greater than 90 dB were documented as having bilateral profound hearing loss. Their parents were then referred by the Department of Otolaryngology for MRI scans with sedation as a presurgical evaluation for CI and consented to participate in our fMRI protocol. SNHL infants who had any malformation or abnormality found in the high-resolution computed tomography scan (HRCT) of the temporal bone or MRI of the brain and inner ear scans were not included in the study. Moreover, all deaf infant participants did not use hearing aids, and had no history of infections, ototoxic drugs, cytomegalovirus, trauma, or any other neural diseases. The control group was well matched to the patient group in terms of age and gender. Participants in the control group received clinical MRI scans with sedation for non-hearing related indications, and their parents agreed to additional sequence scans and hearing tests. Inclusion criteria included: gestational age of at least 36 weeks, no single frequency greater than 25 dB and normal neuroanatomy as determined by a pediatric neuroradiologist. Exclusion criteria included: a variety of central nervous system diseases, such as white matter hypoplasia, abnormal neuronal migration, trauma, tumor, infection, epilepsy, and so on. Signed informed consent was obtained from every patient's parents prior to entering the study. All examinations were approved by the hospital ethics committee.

2.2 | Imaging acquisition

MR images were performed using a Siemens Verio Tim 3.0T MR scanner (Siemens Medical Solutions, Erlangen, Germany) with a 12-channel head coil. All the infants were sedated with 50–60 mg/kg of 10% chloral hydrate orally, 15 min before MR imaging. Hearing protection was provided with earplugs and headphones. During MRI, infants were continuously monitored by a pulse oximeter and closely observed by a pediatrician. All infants underwent anatomical MRI and fMRI acquisitions using the protocol detailed below. The sequence parameters were similar to those reported in our previous study (Wang et al., 2019).

Anatomical MRI consisted of axial and sagittal T1-weighted images (T1WI), as well as axial and coronal T2-weighted images (T2WI) to check for brain lesions and/or abnormalities. Parameters were as follows: T1WI: TR/TE = 300/2.5 ms, slice thickness = 4 mm, interlayer spacing = 1.2 mm, matrix = 320 × 320, FOV = 220 × 220 mm^2, flip angle = 70°, slices covering the whole brain. T2WI: TR/TE = 6000/93 ms, slice thickness = 4 mm, the interlayer spacing = 1.2 mm, matrix = 320 × 320, FOV = 220 × 220 mm^2, flip angle = 120°, slices covering the whole brain.

Resting-state fMRI data were acquired using the echo-planar imaging sequence, with the following parameters: TR/TE = 2000/30 ms, slice thickness = 4 mm, matrix = 70 × 70, FOV = 220 × 220 mm^2, flip angle = 90°, voxel size = 3.1 × 3.1 × 4 mm^3, 30 slices acquired covering the whole brain and total volumes = 190. High-resolution T1-weighted anatomical images were also obtained using a 3D MPRAGE sequence with the following parameters: TR/TE = 2400/3.16 ms, inversion time (TI) = 900 ms, slice thickness = 1 mm, matrix = 224 × 256,

FOV = 220 × 220 mm^2, flip angle = 9°, voxel size = 1.0 × 1.0 × 1.0 mm^3 and 128 sagittal slices covering the whole brain.

2.3 | MRI preprocessing and quality control

The resting-state fMRI data were preprocessed using the Statistical Parametric Mapping (SPM12) software package (http://www.fil.ion. ucl.ac.uk/spm/software/spm12/) and DPARSF toolbox (Chao-Gan, & Yu-Feng, 2010). The first 10 functional volumes were discarded for signal equilibrium and the subjects' adaptation to scanning noise. Slice-timing and realignment for head motion correction were then performed. The reference image for motion correction is the first image. All subjects with a head motion greater than 2.0 mm translation or 2.0° rotation in any direction were excluded. After that, functional images were co-registered to a corresponding T1-weighted high-resolution image. T1-weighted images were segmented using North Carolina University 2-year-old tissue probability maps (Feng et al., 2011). Following that, images were normalized to the 2-year-old brain template (Feng et al., 2011), resampled to 3 mm isotropic voxels, and smoothed with a full width at half-maximum (FWHM) Gaussian Smoothing kernel of 6 mm. Additional preprocessing steps were also conducted to minimize the effect of physiological artifacts on the resting-state signal. These steps including: temporal band-pass filtering (0.01–0.08 Hz), regression of rigid body head motion parameters in six directions, regression of the whole-brain averaged signal, regression of cerebrospinal fluid (CSF) signal averaged from a ventricular region mask, regression of white matter signal averaged from a white matter mask.

Five subjects with head motion of more than 2.0 mm (3 SNHL participants, 2 females; 2 controls, 1 female) were excluded from further analysis. In addition, the first author visually inspected the coregistration and normalization in fMRI data processing in all datasets. As a result, three SNHL participants (1 female, 2 male) failed to coregister structural and functional images, while one control (male) failed to normalize to the 2-year-old brain template. Thus, these nine subjects were excluded from further analyses. In total, 86 subjects (50 SNHL infants and 36 healthy controls) without neuroanatomical anomalies were included in the study. In addition, previous work has shown that frame-to-frame motion has great influence on connectivity results (Power, Barnes, Snyder, Schlaggar, & Petersen, 2012). Frame-wise displacement (FD) was also calculated for assessing the amount of head movement between volumes. We used a volume censoring approach, removing volumes associated with greater than 0.5 mm FD (and one volume before and two volumes after to account for temporal blurring). After that, subjects with less than 114 volumes (60% of the total volumes) were excluded. As a result, no additional subjects were excluded. For the remaining subjects (50 SNHL infants and 36 healthy controls), no significant difference was found in terms of the remaining FD (mm) (mean SNHL = 0.19 (SD = 0.07) vs. mean HC = 0.18 (SD = 0.06), p = .57) and the remaining number of volumes after volume removal (mean SNHL = 161.16 (SD = 16.55) vs. mean HC = 155.01 (SD = 15.81), p = .12) between groups using the Mann–

Whitney U-test. Furthermore, there was no group difference on average volume-by-volume translation (mm) (mean SNHL = 0.92 (SD = 0.43) vs. mean HC = 1.10 (SD = 0.71), p = .34) or rotation (degree) (mean SNHL = 0.41 (SD = 0.28) vs. mean HC = 0.39 (SD = 0.29), p = .67) using Mann–Whitney U-tests (Mayer, Franco, Ling, & Canive, 2007).

2.4 | Independent component analysis

ICA was conducted for all 86 participants, using spatial group-independent component analysis (GICA) framework as implemented in the fMRI Group ICA Toolbox (GIFT; icatb.sourceforge.net, version 2.0) (Allen, Erhardt, Wei, Eichele, & Calhoun, 2012). The mean number of components for all subjects was estimated using the minimum description length criteria for source estimation (Li, Adal, & Calhoun, 2007) and was found to be 38 components. Group ICA was carried out in three stages: (a) data reduction, (b) application of the ICA algorithm, and (c) back-reconstruction for each individual subject. First, data reduction was conducted using principal component analysis (PCA) to reduce the dimensions of the functional data (Calhoun, Adali, Pearlson, & Pekar, 2001). Second, ICA was performed to decompose the grouped data into 38 independent components (ICs) using an Infomax algorithm (Bell & Sejnowski, 1995). This step was repeated 100 times using the ICASSO algorithm for assessing the repeatability or stability of independent components (Himberg et al. 2004). Finally, the ICs for each subject were derived from a GICA back reconstruction step (Calhoun et al., 2001). This provided individual spatial maps and time courses of each IC. Then, for each IC, a group-level T-map was generated and was used to identify the brain regions involved. Group ICA was run treating all subjects as one group to ensure that the same components were identified in each subject. However, to ensure that the same components would be identified in each group, we also ran a group ICA in controls and SNHL separately and identified the same components of interest in each.

We further identified the RSNs of interest based on both temporal characteristics and anatomical localization (visually compared with previously published ICA analyses in youth (Damaraju et al., 2010; de Bie et al., 2012; Gao et al., 2013; Manning, Courchesne, & Fox, 2013) and spatial template-matched with a publically available RSN template derived from ICA analyses in youth (Thomason et al., 2011). Finally, we retained seven RSNs: auditory network (AUN), visual network (VN), sensorimotor network (SMN), default-mode network (DMN), salience network (SN), attention network (AN), and frontal network (FN). They were transformed into z-score maps for further statistical analyses.

2.5 | Network-wise functional connectivity analysis between groups

The intranetwork FC was represented by the z-score of each voxel, which reflects the degree to which the time series of a given voxel

correlates with the mean time series of its corresponding component. First, each RSN was entered into a random-effect one-sample t-test to generate a sample-specific spatial map for each RSN. The sample here referred to both patients and controls. Thresholds were set at $p < .01$ (false discovery rate [FDR] corrected). Next, a two-sample t test was performed to compare the differences in the intra-network FC between the SNHL and control groups. The threshold was set at $p < .05$ (FDR corrected). Gender, age, and head-motion parameters were treated as unconcerned covariates for between-group comparisons.

To measure the interaction between each two RSNs, functional network connectivity (FNC) analyses were performed using the FNC Toolbox (FNC; http://mialab.mrn.org/software/#fnc) (Calhoun et al., 2001). First, subject-specific time courses were detrended and despiked using 3dDespike (http://afni.nimh.nih.gov/afni), then filtered using a fifth-order Butterworth low-pass filter with a high-frequency cut-off of 0.15 Hz. The variance associated with the motion parameter covariates was regressed out. Second, the interaction of each pair of the selected RSNs was evaluated using Pearson's correlation coefficient (r) on the temporally filtered time courses. The FNC toolbox computes a constrained maximal lag correlation between each pair of the selected RSNs by calculating Pearson's correlation coefficient (r) and constraining the lag between the time courses. Maximal lag for the correlation calculation was 4s (2TR). The r value indicates the spontaneous coherence level between RSNs (Jafri et al., 2008). Third, the r value was transformed to z value using Fisher's r-to-z transformation to improve normality for further random-effects between-group analyses. Fourth, significance testing for the inter-network FC within each group and differences between the two groups was carried out using one sample t tests ($p < .05$, FDR corrected) and two-sample t tests ($p < .05$, FDR corrected), respectively. Gender, age, and head-motion parameters were treated as unconcerned covariates for between-group comparisons.

3 | RESULTS

3.1 | Demographic and clinical characteristics

Demographic and clinical data for the subjects are shown in Table 1. No significant differences were found in age and gender between SNHL and control groups. The ABR of the left and right ear were significantly different between two groups.

3.2 | Identifications of the resting-state networks

The group ICA approach automatically generated 38 ICs. Back-reconstruction of spatial networks to individual subjects shows strong similarity between the SNHL and HC groups (Figure S1 in the Supplement). Among the 38 components, 19 components (seven RSNs) were selected as the focus of subsequent analysis (Figure 1). These networks include: an auditory network (AUN) (ICs 15, 25)

	SNHL group	HC group	P value
Number (n)	50	36	—
Age (months)[a] (mean ± SD)	17.69 ± 6.88	18.59 ± 7.36	.57
Age range (months)	9–36	9–36	—
Gender (male/female)[b]	23/27	17/19	.79
ABR of left ear (dB HL) (mean ± SD)	>90	21.36 ± 2.46	—
ABR of right ear (dB HL) (mean ± SD)	>90	21.66 ± 2.53	—

TABLE 1 Demographic and clinical data of all subjects

Abbreviations: ABR, auditory brainstem response; HC, health control; SD, standard deviation; SNHL, sensorineural hearing loss.
[a]Statistical analyses for comparisons between groups were carried out with t-tests.
[b]Statistical analyses for comparisons between groups were carried out with χ^2 tests.

consisted of bilateral insula, middle temporal gyrus and superior temporal gyrus; a visual network (VN) (ICs 3, 6, 7, 8, 9, and 26) consisted of bilateral calcarine, cuneus, lingual gyrus, and superior, middle and inferior occipital gyri; a sensorimotor network (SMN) (ICs 21, 32, 36) consisted of bilateral paracentral lobule; a default mode network (DMN) (ICs 10 and 22) consisted of posterior cingulate cortex, bilateral inferior parietal cortex, and precuneus; a salience network (SN) (ICs ICs 34, 35) consisted of anterior cingulate cortex and bilateral insula; an attention network (AN) (ICs 17, 23, 29) consisted of bilateral intraparietal sulcus, inferior parietal lobule, superior parietal lobule; a frontal network (FN) (IC 37) consisted of bilateral dorsal frontal cortex.

3.3 | Intranetwork functional connectivity changes between groups

Compared to HC, SNHL group showed decreased FC in the right inferior parietal lobule within DMN (p < .05, FDR corrected), increased FC in the left superior temporal gyrus (STG) within AUN (p < .05, FDR corrected), increased FC in the left parahippocampal gyrus and right anterior cingulate cortex within SN (p < .05, FDR corrected) (Table 2; Figure 2). The AN, SMN, VN, FN did not reveal significant group difference.

3.4 | Internetwork functional connectivity changes between groups

The results of one-sample t-tests (p < .05, FDR corrected) showed within-group internetwork correlations in two groups (Figure 3).

Further inter-group differences (SNHL–HC) were presented in Figure 4a. In total, 210 comparisons were made between networks. Of these comparisons, significant increased connections were found in SNHL group compared with the controls for four network comparisons (p < .05, FDR corrected). These increased connections were between SMN (IC21) and AUN (IC15), FN (IC37) and AUN (IC15), SMN (IC36) and VN (IC26), as well as the FN (IC37) and VN (IC26). A circular connectivity plot (Figure 4b) shows significant between-group differences.

There was a significant anticorrelation in control group between SMN (IC21) and AUN (IC15), FN (IC37) and AUN (IC15), SMN (IC36) and VN (IC26), whereas there was no significant correlation for the SNHL group. The FN (IC37) and VN (IC26) connection represented significantly positive correlations within the SNHL group, whereas no significant correlation was observed in controls.

4 | DISCUSSION

In this study, seven RSNs were identified using data-driven ICA in both SNHL and control groups. Group comparison demonstrated increased FC within the AUN and SN as well as decreased connectivity within the DMN in SNHL group. Further, increased internetwork FCs (SMN–AUN, FN–AUN, VN–SMN, and VN–FN) were detected in SNHL group. These findings suggested that the absence of auditory stimuli during early sensitive period leads to both decreased FC and compensatory plasticity in both intra- and inter-RSNs. By focusing on the relatively narrow age range of 9–36 months, these findings fill a gap in our understanding of the FC changes of early auditory deprivation that occur specifically during this specific developmental window.

4.1 | Increased intranetwork functional connectivity within the auditory network

The auditory network is one of the reliably observed as well as the earliest recognizable brain networks, even though not yet extensively studied. It appeared in the third month of embryo, that is, the most rapid period of fetal neural development (Thomason et al., 2013). Its FC increases linearly with age (Rohr et al., 2018), until adulthood. This network encompasses primary auditory cortices including Heschl's gyrus, superior temporal gyri, insula, cingulate, post- and pre-central gyri, and supramarginal gyrus (Beckmann et al., 2005; Laird et al., 2011; Smith et al., 2009). Sensory deprivation, as in congenital profound SNHL, can dramatically alter functional connectivity and growth in the auditory system. In a study of deaf cats (Wong, Chabot, Kok, & Lomber, 2014), the researchers found that the auditory cortex of early deafness cats had significant changes in regional mapping, but not in late deafness cats, indicating that the time of deafness had an
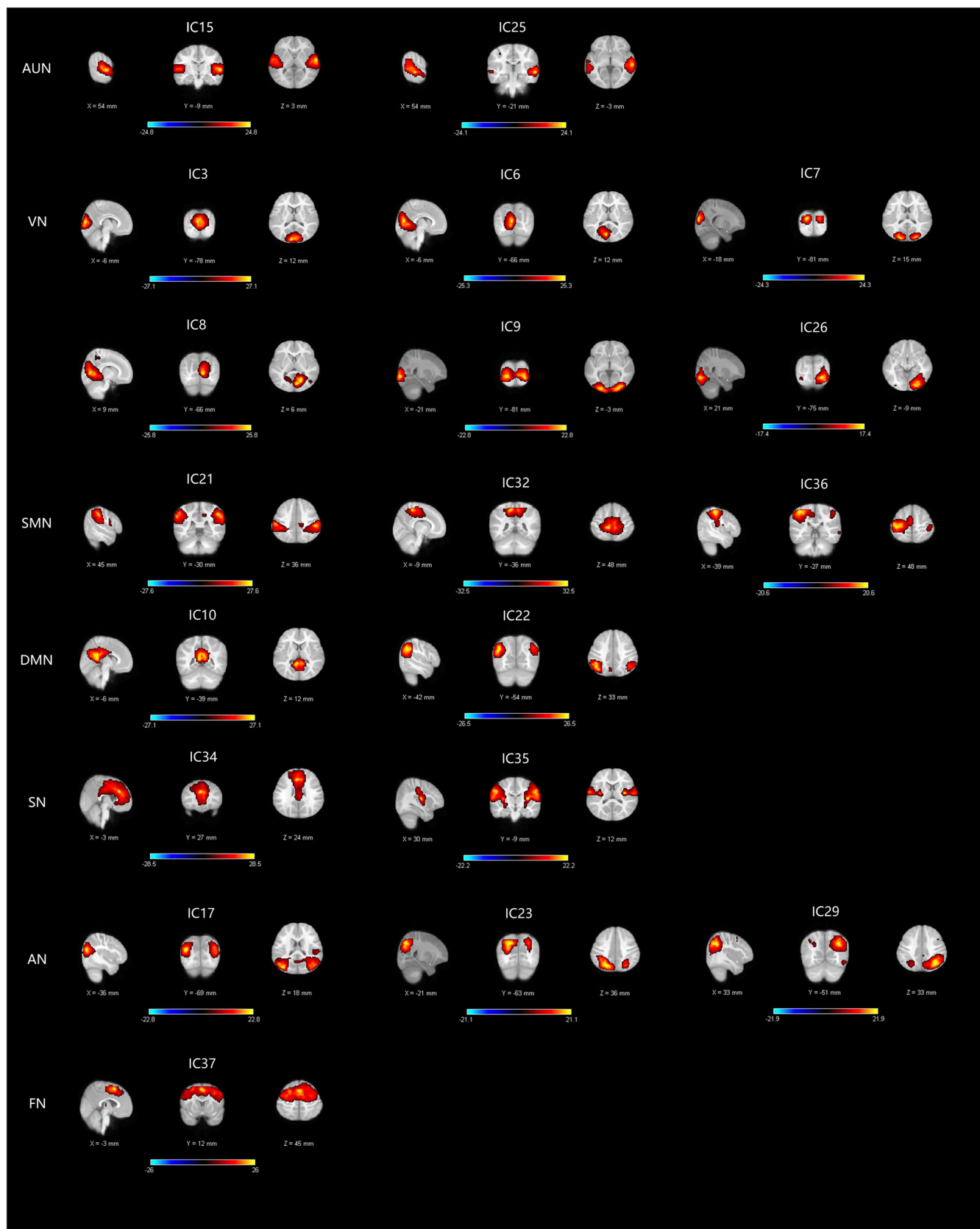
FIGURE 1 Functional relevant resting-state networks (RSNs). The spatial maps of 19 independent components (ICs) were selected as the RSNs for further analysis. The color scale represents the *t* values in each IC. Images are over-laid on the 2-year-old brain template. The brains are displayed in radiological orientation (i.e., left is right). AN, attention network; AUN, auditory network; DMN, default mode network; FN, frontal network; SMN, sensorimotor network; SN, salience network; VN, visual network

Brain region (2-year-old AAL template)	RSN	Voxel size	Peak z values	Coordinates x, y, z
SNHL < HC				
Inferior parietal lobule, R	DMN	10	3.28	51, −54, 18
SNHL > HC				
Superior temporal gyrus, L	AN	25	4.89	−53, 3, −8
Parahippocampal gyrus, L	SN	10	4.52	−27, −18, −15
Anterior cingulate cortex, R	SN	25	4.21	6, 46, 12
Anterior cingulate cortex, R	SN	15	3.77	11, 33, 27

Note: Coordinates (x, y, z) are in North Carolina University 2-year-old brain template. Results are shown at $p < .05$, false discovery rate (FDR) corrected, adjusting for age, sex and motion parameters.
Abbreviations: AAL, anatomical automatic labeling; AN, auditory network; DMN, default mode network; HC, healthy controls; L, left hemisphere; R, right hemisphere; RSN, resting-state networks; SN, salience network; SNHL, sensorineural hearing loss.

important impact on the development of the auditory cortex. In this study, we found that FC within the left STG of the AUN was stronger in SNHL group. It might indicate that a compensatory reorganization of the AUN had occurred within early development sensitive period to limit the consequences of early auditory deprivation. STG is essential for basic acoustic analysis (Hickok, 2012). This area also shows consistent differences across studies of neuroanatomical differences in the hearing impaired, although these studies tend to focus on adults with prolonged hearing impairment (Shibata, 2007; Smith et al., 2011). Feng and colleagues analyzed pre-CI neural morphological data obtained from MRI in SNHL patients younger than 3.5 years (Feng et al., 2018). They found the most obvious neuro-morphological differences between the SNHL patients and NH groups lie in the bilateral auditory cortex, especially the middle portion of STG. Therefore, the increased FC within AUN found in our study may indicating a kind of functional compensation for the morphologic changes in regions related to auditory.

4.2 | Decreased intranetwork functional connectivity within the DMN

Early childhood is a particularly crucial period in a child's development when many cognitive skills are rapidly maturing. The DMN is known to be a network closely related to the integration of cognitive and emotional processing, that is, in internally directed mental activity, thoughts and monitoring of the world around us (Buckner, Andrews-Hanna, & Schacter, 2008). It is one of the first higher order networks to show a well-distributed network structure by integrating distant medial frontal, medial/lateral parietal, and medial/lateral temporal regions starting at 6 months of age (Gao, Lin, Grewen, & Gilmore, 2016). The default network topology at 1 year of age resembles an adult-like organization, consistent with the concurrent emergence of the corresponding cognitive functions (Gao et al., 2013). The newest research demonstrates that human vigilance can be directly related to the activity of the DMN (Hinds et al., 2013) and an atypical

pattern in DMN can be associated with attention impairments (Bonnelle et al., 2011; Broyd et al., 2009; Mee Bell, Mccallum, & Cox, 2003). In this study, SNHL group showed reduced FC in the right inferior parietal lobule of the DMN. The inferior parietal lobule is one of the main nodes of the DMN, which has been implicated in social perception, judgment, and self-referential processing (Uddin, Kelly, Biswal, Castellanos, & Milham, 2009). It may indicate delayed or abnormal development of the FC within the DMN.

However, it should be noted that our finding is inconsistent with the previous reports that the patients with hearing loss presented increased FC in the DMN (Husain et al., 2014; Wang et al., 2014; Zhang et al., 2015). The possible reason for this inconsistency might be that the previous study subjects were middle-aged adults with a long history of hearing loss, while we focused on SNHL children under the age of three, who were still within early sensitive period. At this stage, the DMN is still in the process of rapid development (Damaraju et al., 2014; Gao et al., 2016). Therefore, this study suggests that the absence of early auditory stimulation within early sensitive period may result in delayed or abnormal development of the FC within the DMN rather than compensatory reorganization induced by long-term hearing loss.

4.3 | Increased intranetwork functional connectivity within the salience network

The salience network, which is important for the initiation of cognitive control, consists of the dorsal anterior cingulate cortex (ACC) and bilateral anterior insula, with robust connectivity to subcortical and limbic structures. It is activated by conditions, which require a rapid change in behavior, particularly errors and signals the need for behavior adaptation (Seeley et al., 2007). The role of the SN seems to be a mediator of the function of other networks. Further, the same regions are also activated in response to pain, uncertainty, and threats to homeostasis; that is, events and experiences with a high degree of personal salience (Menon & Uddin, 2010). Song et al. (2015)
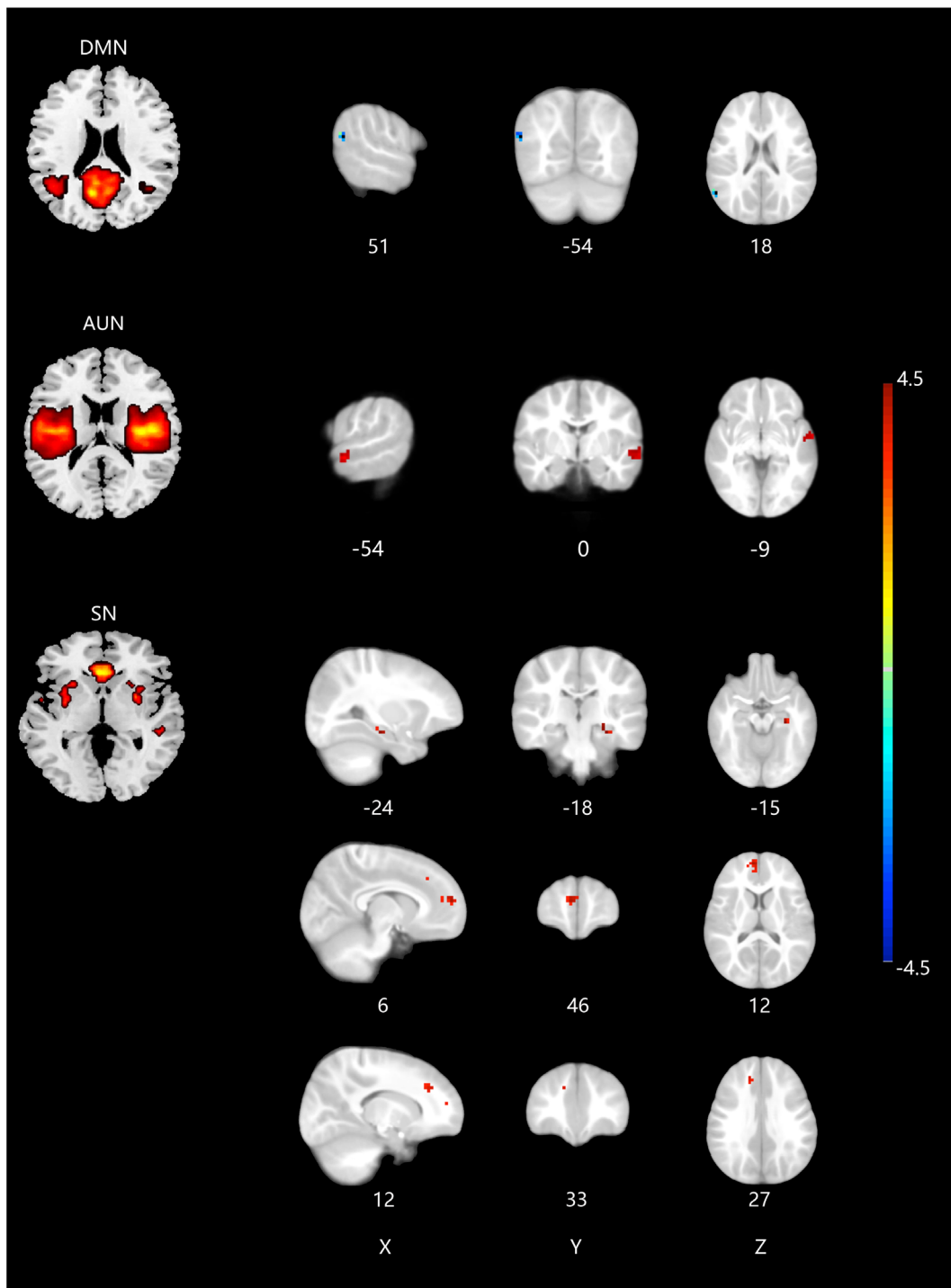
FIGURE 2 Regions where SNHL patients showed decreased (cold colors) or increased (warm colors) functional connectivity within the resting-state networks compared to healthy controls. All images were shown with FDR correction of *p* < .05. The colored bar indicates the corresponding *t* values. Images are over-laid on the 2-year-old brain template. The brains are displayed in radiological orientation (i.e., left is right). AUN, auditory network; DMN, default mode network; FDR, false discovery rate; SN, salience network; SNHL, sensorineural hearing loss

performed activation likelihood estimation meta-analysis of positron emission tomography (PET) studies in CI users and normal hearing controls, found that, for both the lexical stimuli and nonlexical stimuli, significant activations were observed in areas comprising SN in the CI user group. It is suggested that dual-stream auditory processing in CI

users may need extra supports from the SN to cope with degraded auditory signal provided by the implant. Our findings of increased connectivities in the SN showed in SNHL group may be related to the abnormal detection or processing of external information in children with no auditory stimulation, and was also in accordance with the
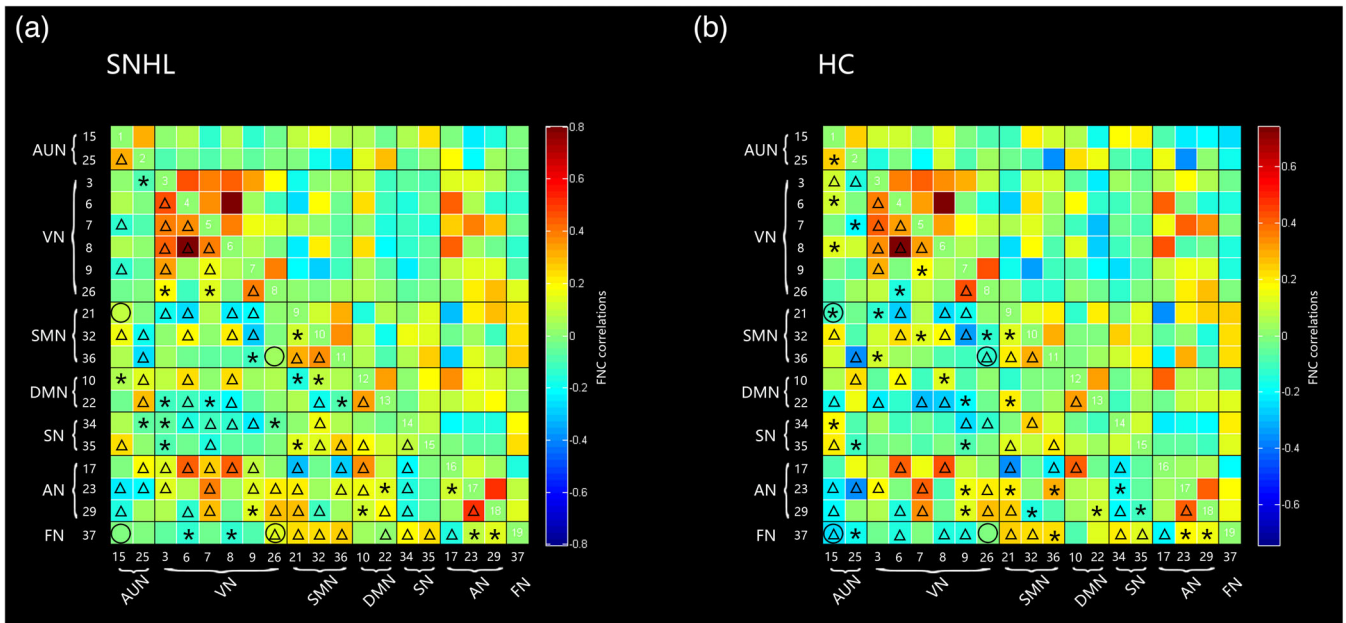
FIGURE 3 The functional connectivity correlation matrix between all RSNs within SNHL group (a) and HC group (b). The color scale represents the value of the correlations; Warm color represents positive correlations, cold color represents anti-correlations. The markers indicate significant functional connection between networks (*$p < .05$, FDR corrected; $\Delta p < .01$, FDR corrected). Circles overlying network comparisons indicate significant between-group differences (also see Figure 4). AN, attention network; AUN, auditory network; DMN, default mode network; HC, healthy controls; FDR, false discovery rate; FN, frontal network; FNC, functional network connectivity; VN, visual network; RSN, resting-state networks; SMN, sensorimotor network; SN, salience network; SNHL, sensorineural hearing loss
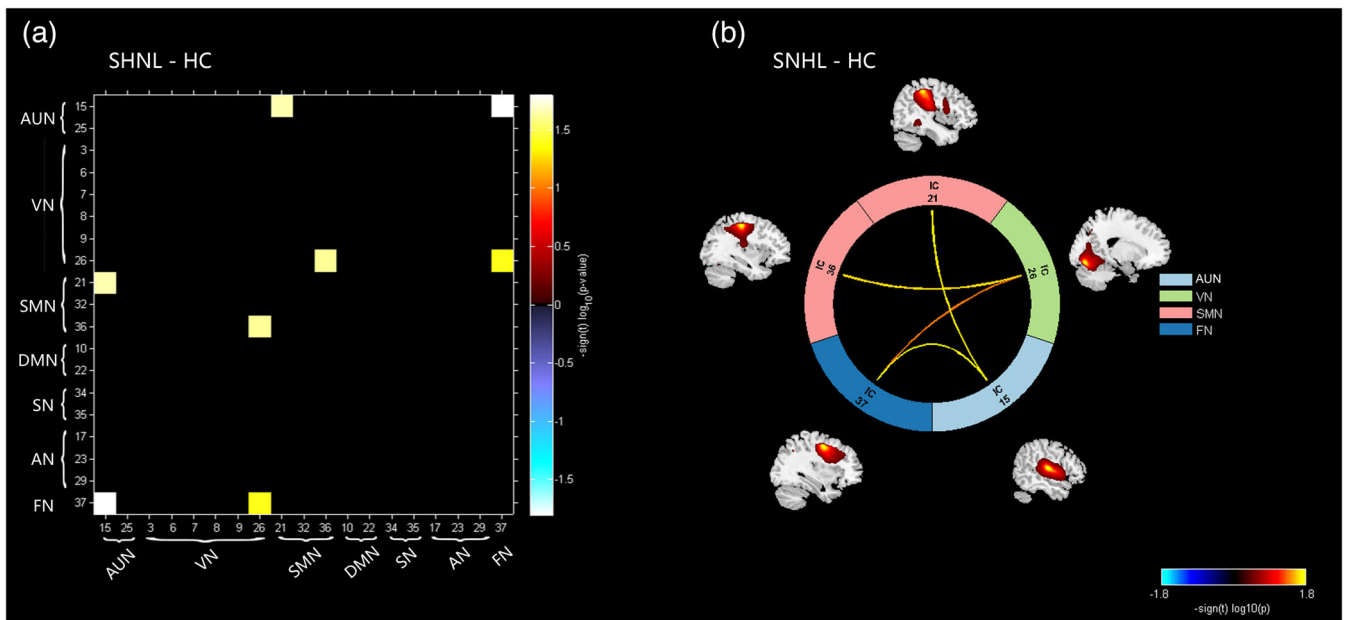

FIGURE 4 (a) Matrix shows differences of internetwork functional connectivity between two groups. (b) Significance and direction following two-sample t-tests (SNHL-HC) on each pairwise correlation are depicted as the $-\text{sign}(t\,\text{val})\log10(p\,\text{val})$. Significant differences from panel A are shown on a circle plot between networks. Color of the lines connecting the networks is scaled to the color bar. Compared with the controls, SNHL group showed increased connections between SMN (IC21) and AUN (IC15), FN (IC37) and AUN (IC15), SMN (IC36) and VN (IC26), as well as the FN (IC37) and VN (IC26) ($p < .05$, FDR corrected). AN, attention network; AUN, auditory network; DMN, default mode network; FDR, false discovery rate; FN, frontal network; HC, healthy controls; IC, independent component; SMN, sensorimotor network; SN, salience network; SNHL, sensorineural hearing loss; VN, visual network

clinical high alert state of deaf patients (Moon, Park, Jung, Lee, & Lee, 2018; Stevens, Dubno, Wallhagen, & Tucci, 2019).

Parahippocampus gyrus, also part of the limbic system, played a pivotal role not only in the cognitive processing but also in the process of memory retrieval and attention. Furthermore, the limbic system is considered to be involved in the reception of auditory signals and the process of appropriate response (Blaizot et al., 2010). Our findings of increased FC in parahippocampus gyrus may support the hypothesis that the brain regions associated with auditory perception are reorganized to improve sensitivity to auditory stimuli in SNHL patients within early sensitive period.

4.4 | Increased internetwork functional connectivity among networks

The brain is a complex network consisting of multiple RSNs serving different functions. These RSNs have complex antagonistic and integrated relationships to maintain efficient brain function. Analyzing connectivity strength among RSNs might be a valuable tool to assess the functional changes corresponding to SNHL and contribute to our understanding of the overall brain activity changes after early auditory deprivation. Previous neuroimaging studies have shown that, if hearing is not established during sensitive periods in development, the auditory brain vulnerable to cross-modal recruitment by the visual (Heggdal, Brännström, Aarstad, Vassbotn, & Specht, 2016; Schmithorst, Plante, & Holland, 2014; Wang et al., 2014; Yang et al., 2014) and somatosensory systems (Meredith, Clemo, Chabot, et al., 2016; Clemo, Lomber, & Meredith, 2016). In this study, SNHL group showed increased internetwork FC between SMN (IC21) and AUN (IC15), FN (IC37) and AUN (15), SMN (IC36) and VN (IC26), FN (IC37) and VN (IC26). It was suggesting that auditory deprivation might have begun to affect functional connectivity in cross-modal and general cognitive brain regions.

In many cases, cortical modifications allow multisensory cortices to recruit available auditory regions for enhanced visual and/or somatosensory processing, at the expense of auditory processing abilities (Kral, Hubka, Heid, & Tillein, 2013; Kral & Sharma, 2012). The auditory cortex shows activation to somatosensory stimuli in older adult patients with moderate hearing loss (Cardon & Sharma, 2018) and in late cochlear implanted children (Sharma et al., 2015). Furthermore, such cross-modal reorganization may be related to less than optimal outcomes with the cochlear implant. In the current study, the FC between SMN (IC21) and AUN (IC15), SMN (IC36) and VN (IC26) were found to be significantly anti-correlated in control group, but not significantly correlated in SNHL group. It may suggested that the weakening of the function of the auditory system, due to diminished input, could lead to alterations of multisensory connections. Further reflected neuroplastic changes involved in mediating auditory-somatosensory and visual-somatosensory interactions, which might be an early functional coupling pattern of the cross-modality.

The increased FC between the FN (IC37) and AUN (15), FN (IC37), and VN (IC26) may indicate a more significant role of FN in

auditory and visual processing in deaf patients. It might be a product of a compensatory underlying process in cortical development to compensate for the decline of auditory and cognitive abilities in the SNHL patients within early sensitive period. In addition, the increased FC between the primary sensory network and the advanced cognitive network is also related to the good outcomes after CI (Deshpande, Tan, Lu, Altaye, & Holland, 2016; Giraud & Lee, 2007). Thus, our results may be part of the functional basis explaining the most optimal outcomes of CI carried out within early sensitive period.

4.5 | Limitations

The primary limitation of this study was the small sample size of infants. By focusing on the relatively narrow age range of 9–36 months, we are better able to capture the detailed changes that occur specifically during this special period. However, to provide an overall view of the brain development after early auditory deprivation, a study including samples covering a larger age range is needed. A larger sample size may enable a finer division of age ranges (e.g., every 6 months). Combined with the age-appropriate tissue probability templates, it would facilitate the acquisition of more detailed brain development trajectory after early auditory deprivation. Secondly, our article did not involve the analysis of morphological images. Previous studies using voxel-based morphometry (VBM) analysis suggested that significant morphological changes exist in region of the auditory cortex as a result of auditory deprivation in adults (Shibata, 2007), infants by 1 year of age (Smith et al., 2011) and infants by 3.5 years of age (Feng et al., 2018). Feng et al. (2018) further found regions in the auditory association and cognitive networks to be most predictive of future speech-perception development. It is a big step toward the goal of personalized therapy for children with CI. In the future, the combination of both functional and morphological analysis may have vast potential for exploring imaging markers to predict the prognosis of CI. Thirdly, clinical information about the auditory and language function recovery after CI was in the process of follow-up. The correlation between the recovery and abnormal brain network connectivity in infants with SNHL prior to CI needs to be investigated in the future study.

5 | CONCLUSION

This study used group ICA to assess the intra- and inter-network FC characteristics in profound SNHL within early sensitive period. It was found that, compared with the control group, SNHL group showed decreased FC within DMN while increased FC within auditory and salience network. Further, enhanced inter-network FC between SMN–AUN, FN–AUN, SMN–VN, FN–VN were also found in SNHL group. These results support the idea that both functional connectivity loss and compensatory reorganization occur following early life auditory deprivation. It provides further evidence for understanding

the brain network maturational trajectory after hearing loss in the early sensitive period.

ORCID

Guoguang Fan https://orcid.org/0000-0001-8114-5727

REFERENCES

Allen, E. A., Erhardt, E. B., Wei, Y., Eichele, T., & Calhoun, V. D. (2012). Capturing inter-subject variability with group independent component analysis of fMRI data: A simulation study. *NeuroImage*, *59*(4), 4141–4159.

Beckmann, C. F., Deluca, M., Devlin, J. T., & Smith, S. M. (2005). Investigations into resting-state connectivity using independent component analysis. *Philosophical Transactions Biological Sciences*, *360*(1457), 1001–1013.

Bell, A. J., & Sejnowski, T. J. (1995). An information-maximization approach to blind separation and blind deconvolution. *Neural Computation*, *7*(6), 1129–1159.

Biswal, B. B., Van Kylen, J., & Hyde, J. S. (1997). Simultaneous assessment of flow and BOLD signals in resting-state functional connectivity maps. *NMR in Biomedicine*, *10*(4–5), 165–170. https://doi.org/10.1002/(sici)1099-1492(199706/08)10:4/5<165::aid-nbm454>3.0.co;2-7

Blaizot, X., Mansilla, F., Insausti, A. M., Constans, J. M., Salinasalamán, A., Prósistiaga, P., ... Insausti, R. (2010). The human Parahippocampal region: I. temporal pole Cytoarchitectonic and MRI correlation. *Cerebral Cortex*, *20*(9), 2198.

Bonnelle, V., Leech, R., Kinnunen, K. M., Ham, T. E., Beckmann, C. F., De Boissezon, X., ... Sharp, D. J. (2011). Default mode network connectivity predicts sustained attention deficits after traumatic brain injury. *Journal of Neuroscience*, *31*(38), 13442–13451. https://doi.org/10.1523/JNEUROSCI.1163-11.2011

Broyd, S. J., Demanuele, C., Debener, S., Helps, S. K., James, C. J., & Sonuga-Barke, E. J. S. (2009). Default-mode brain dysfunction in mental disorders: A systematic review. *Neuroscience & Biobehavioral Reviews*, *33*(3), 279–296.

Buckner, R. L., Andrews-Hanna, J. R., & Schacter, D. L. (2008). The brain's default network: Anatomy, function, and relevance to disease. *Annals of the New York Academy of Sciences*, *1124*, 1–38. https://doi.org/10.1196/annals.1440.011

Calhoun, V., Adali, T., Pearlson, G., & Pekar, J. (2001). A method for making group inferences using independent component analysis of functional MRI data: Exploring the visual system. *NeuroImage*, *13*(6), 88–88.

Calhoun, V. D., & Adali, T. (2006). Unmixing fMRI with independent component analysis. *Engineering in Medicine & Biology Magazine IEEE*, *25*(2), 79–90.

Cardon, G., & Sharma, A. (2018). Somatosensory cross-modal reorganization in adults with age-related, early-stage hearing loss. *Frontiers in Neuroscience*, *12*, 172. https://doi.org/10.3389/fnhum.2018.00172

Chen, M. M., & Oghalai, J. S. (2016). Diagnosis and Management of Congenital Sensorineural Hearing Loss. *Curr Treat Options Pediatr*, *2*(3), 256–265. https://doi.org/10.1007/s40746-016-0056-6

Chao-Gan, Y., & Yu-Feng, Z. (2010). DPARSF: A MATLAB toolbox for "pipeline" data analysis of resting-state fMRI. *Frontiers in System Neuroscience*. *4*, 13. https://doi.org/10.3389/fnsys.2010.00013

Clemo, H. R., Lomber, S. G., & Meredith, M. A. (2016). Synaptic basis for cross-modal plasticity: Enhanced supragranular dendritic spine density in anterior ectosylvian auditory cortex of the early deaf cat. *Cerebral Cortex*, *26*(4), 1365–1376. https://doi.org/10.1093/cercor/bhu225

Cordes, D., Haughton, V. M., Arfanakis, K., Carew, J. D., Turski, P. A., Moritz, C. H., ... Meyerand, M. E. (2001). Frequencies contributing to functional connectivity in the cerebral cortex in "resting-state" data. *AJNR. American Journal of Neuroradiology*, *22*(7), 1326–1333.

Damaraju, E., Caprihan, A., Lowe, J. R., Allen, E. A., Calhoun, V. D., & Phillips, J. P. (2014). Functional connectivity in the developing brain: A longitudinal study from 4 to 9months of age. *NeuroImage*, *84*, 169–180. https://doi.org/10.1016/j.neuroimage.2013.08.038

Damaraju, E., Phillips, J. R., Lowe, J. R., Ohls, R., Calhoun, V. D., & Caprihan, A. (2010). Resting-state functional connectivity differences in premature children. *Frontiers in Systems Neuroscience*, *4*, 23. https://doi.org/10.3389/fnsys.2010.00023

de Bie, H. M., Boersma, M., Adriaanse, S., Veltman, D. J., Wink, A. M., Roosendaal, S. D., ... Sanz-Arigita, E. J. (2012). Resting-state networks in awake five- to eight-year old children. *Human Brain Mapping*, *33*(5), 1189–1201. https://doi.org/10.1002/hbm.21280

De, L. M., Beckmann, C. F., De, S. N., Matthews, P. M., & Smith, S. M. (2006). fMRI resting state networks define distinct modes of long-distance interactions in the human brain. *NeuroImage*, *29*(4), 1359–1367.

Deshpande, A. K., Tan, L., Lu, L. J., Altaye, M., & Holland, S. K. (2016). fMRI as a Preimplant objective tool to predict postimplant oral language outcomes in children with cochlear implants. *Ear and Hearing*, *37*(4), e263–e272. https://doi.org/10.1097/AUD.0000000000000259

Feng, G., Ingvalson, E. M., Grieco-Calub, T. M., Roberts, M. Y., Ryan, M. E., Birmingham, P., ... Wong, P. C. M. (2018). Neural preservation underlies speech improvement from auditory deprivation in young cochlear implant recipients. *Proceedings of the National Academy of Sciences*, *115*(5), E1022–E1031. https://doi.org/10.1073/pnas.1717603115

Feng, S., Yap, P. T., Wu, G., Jia, H., Gilmore, J. H., Lin, W., & Shen, D. (2011). Infant brain atlases from neonates to 1- and 2-year-olds. *PLoS One*, *6*(4), e18746.

Fox, M. D., & Raichle, M. E. (2007). Spontaneous fluctuations in brain activity observed with functional magnetic resonance imaging. *Nature Reviews Neuroscience*, *8*(9), 700–711.

Gao, W., Gilmore, J. H., Shen, D., Smith, J. K., Zhu, H., & Lin, W. (2013). The synchronization within and interaction between the default and dorsal attention networks in early infancy. *Cerebral Cortex*, *23*(3), 594–603.

Gao, W., Lin, W., Grewen, K., & Gilmore, J. H. (2016). Functional connectivity of the infant human brain. *The Neuroscientist*, *23*(2), 169–184. https://doi.org/10.1177/1073858416635986

Giraud, A. L., & Lee, H. J. (2007). Predicting cochlear implant outcome from brain organisation in the deaf. *Restorative Neurology & Neuroscience*, *25*(3–4), 381–390.

Heggdal, P. O. L., Brännström, J., Aarstad, H. J., Vassbotn, F. S., & Specht, K. (2016). Functional-structural reorganisation of the neuronal network for auditory perception in subjects with unilateral hearing loss: Review of neuroimaging studies. *Hearing Research.*, *332*, 73–79.

Hickok, G. (2012). The cortical organization of speech processing: Feedback control and predictive coding the context of a dual-stream model. *Journal of Communication Disorders*, *45*(6), 393–402.

Himberg, J., Hyvarinen, A., & Esposito, F. (2004). Validating the independent components of neuroimaging time-series via clustering and visualization. *Neuroimage*, *22*, 1214–1222.

Hinds, O., Thompson, T. W., Ghosh, S., Yoo, J. J., Whitfieldgabrieli, S., Triantafyllou, C., & Gabrieli, J. D. (2013). Roles of default-mode network and supplementary motor area in human vigilance performance: Evidence from real-time fMRI. *Journal of Neurophysiology*, *109*(5), 1250–1258.

Huang, L., Zheng, W., Wu, C., Wei, X., Wu, X., Wang, Y., & Zheng, H. (2015). Diffusion tensor imaging of the auditory neural pathway for clinical outcome of cochlear implantation in pediatric congenital sensorineural hearing loss patients. *PLoS One*, *10*(10), e0140643. https://doi.org/10.1371/journal.pone.0140643

Husain, F. T., Carpenter-Thompson, J. R., & Schmidt, S. A. (2014). The effect of mild-to-moderate hearing loss on auditory and emotion processing networks. *Frontiers in Systems Neuroscience*, *8*, 10. https://doi.org/10.3389/fnsys.2014.00010

Jafri, M. J., Pearlson, G. D., Stevens, M., & Calhoun, V. D. (2008). A method for functional network connectivity among spatially independent resting-state components in schizophrenia. *NeuroImage*, *39*(4), 1666–1681.

Jung, M. E., Colletta, M., Coalson, R., Schlaggar, B. L., & Lieu, J. E. C. (2017). Differences in interregional brain connectivity in children with unilateral hearing loss. *Laryngoscope*, *127*(11), 2636–2645. https://doi.org/10.1002/lary.26587

Kral, A., Hubka, P., Heid, S., & Tillein, J. (2013). Single-sided deafness leads to unilateral aural preference within an early sensitive period. *Brain*, *136*(Pt 1), 180–193. https://doi.org/10.1093/brain/aws305

Kral, A., & O'Donoghue, G. M. (2010). Profound deafness in childhood. *The New England Journal of Medicine*, *363*(15), 1438–1450. https://doi.org/10.1056/NEJMra0911225

Kral, A., & Sharma, A. (2012). Developmental neuroplasticity after cochlear implantation. *Trends in Neurosciences*, *35*(2), 111–122. https://doi.org/10.1016/j.tins.2011.09.004

Laird, A. R., Fox, P. M., Eickhoff, S. B., Turner, J. A., Ray, K. L., Mckay, D. R., ... Fox, P. T. (2011). Behavioral interpretations of intrinsic connectivity networks. *Journal of Cognitive Neuroscience*, *23*(12), 4022–4037.

Li, Y., Booth, J. R., Peng, D., Zang, Y., Li, J., Yan, C., & Ding, G. (2013). Altered intra- and inter-regional synchronization of superior temporal cortex in deaf people. *Cerebral Cortex*, *23*(8), 1988–1996. https://doi.org/10.1093/cercor/bhs185

Li, Y. O., Adal, T., & Calhoun, V. D. (2007). Estimating the number of independent components for functional magnetic resonance imaging data. *Human Brain Mapping*, *28*(11), 1251–1266.

Liu, B., Feng, Y., Yang, M., Chen, J. Y., Li, J., Huang, Z. C., & Zhang, L. L. (2015). Functional connectivity in patients with sensorineural hearing loss using resting-state MRI. *American Journal of Audiology*, *24*(2), 145–152. https://doi.org/10.1044/2015_AJA-13-0068

Luan, Y., Wang, C., Jiao, Y., Tang, T., Zhang, J., & Teng, G.-J. (2019). Dysconnectivity of multiple resting-state networks associated with higher-order functions in sensorineural hearing loss. *Frontiers in Neuroscience*, *13*, 55. https://doi.org/10.3389/fnins.2019.00055

Manning, J. H., Courchesne, E., & Fox, P. T. (2013). Intrinsic connectivity network mapping in young children during natural sleep. *NeuroImage*, *83*, 288–293. https://doi.org/10.1016/j.neuroimage.2013.05.020

Mayer, A. R., Franco, A. R., Ling, J., & Canive, J. M. (2007). Assessment and quantification of head motion in neuropsychiatric functional imaging research as applied to schizophrenia. *Journal of the International Neuropsychological Society*, *13*(5), 839–845. https://doi.org/10.1017/S1355617707071081

Mee Bell, S., Mccallum, R. S., & Cox, E. A. (2003). Toward a research-based assessment of dyslexia: Using cognitive measures to identify reading disabilities. *Journal of Learning Disabilities*, *36*(6), 505–516.

Menon, V., & Uddin, L. Q. (2010). Saliency, switching, attention and control: A network model of insula function. *Brain Structure and Function*, *214*(5-6), 655–667. https://doi.org/10.1007/s00429-010-0262-0

Meredith, M. A., Clemo, H. R., Corley, S. B., Chabot, N., & Lomber, S. G. (2016). Cortical and thalamic connectivity of the auditory anterior ectosylvian cortex of early-deaf cats: Implications for neural mechanisms of crossmodal plasticity. *Hearing Research*, *333*, 25–36. https://doi.org/10.1016/j.heares.2015.12.007

Mongerson, C. R. L., Jennings, R. W., Borsook, D., Becerra, L., & Bajic, D. (2017). Resting-state functional connectivity in the infant brain: Methods, pitfalls, and potentiality. *Frontiers in Pediatrics*, *5*, 159. https://doi.org/10.3389/fped.2017.00159

Moon, K. R., Park, S., Jung, Y., Lee, A., & Lee, J. H. (2018). Effects of anxiety sensitivity and hearing loss on tinnitus symptom severity. *Psychiatry Investigation*, *15*(1), 34–40.

Power, J. D., Barnes, K. A., Snyder, A. Z., Schlaggar, B. L., & Petersen, S. E. (2012). Spurious but systematic correlations in functional connectivity MRI networks arise from subject motion. *NeuroImage*, *59*(3), 2142–2154. https://doi.org/10.1016/j.neuroimage.2011.10.018

Propst, E. J., & Greinwald, J. V. (2010). Neuroanatomic differences in children with unilateral sensorineural hearing loss detected using functional magnetic resonance imaging. *Archives of Otolaryngology – Head & Neck Surgery*, *136*(1), 22–26.

Rohr, C. S., Arora, A., Cho, I. Y. K., Katlariwala, P., Dimond, D., Dewey, D., & Bray, S. (2018). Functional network integration and attention skills in young children. *Developmental Cognitive Neuroscience*, *30*, 200–211. https://doi.org/10.1016/j.dcn.2018.03.007

Schmithorst, V. J., Plante, E., & Holland, S. (2014). Unilateral deafness in children affects development of multi-modal modulation and default mode networks. *Frontiers in Human Neuroscience*, *8*, 164. https://doi.org/10.3389/fnhum.2014.00164

Seeley, W. W., Menon, V., Schatzberg, A. F., Keller, J., Glover, G. H., Kenna, H., ... Greicius, M. D. (2007). Dissociable intrinsic connectivity networks for salience processing and executive control. *Journal of Neuroscience*, *27*(9), 2349–2356.

Sharma, A., & Campbell, J. (2011). A sensitive period for cochlear implantation in deaf children. *The Journal of Maternal-Fetal & Neonatal Medicine*, *24*(Suppl 1), 151–153. https://doi.org/10.3109/14767058.2011.607614

Sharma, A., Campbell, J., & Cardon, G. (2015). Developmental and crossmodal plasticity in deafness: Evidence from the P1 and N1 event related potentials in cochlear implanted children. *International Journal of Psychophysiology*, *95*(2), 135–144. https://doi.org/10.1016/j.ijpsycho.2014.04.007

Shi, B., Yang, L. Z., Liu, Y., Zhao, S. L., Wang, Y., Gu, F., ... Zhang, X. (2016). Early-onset hearing loss reorganizes the visual and auditory network in children without cochlear implantation. *Neuroreport*, *27*(3), 197–202. https://doi.org/10.1097/WNR.0000000000000524

Shibata, D. K. (2007). Differences in brain structure in deaf persons on MR imaging studied with voxel-based morphometry. *Ajnr American Journal of Neuroradiology*, *28*(2), 243–249.

Smith, K. M., Mecoli, M. D., Altaye, M., Komlos, M., Maitra, R., Eaton, K. P., ... Holland, S. K. (2011). Morphometric differences in the Heschl's gyrus of hearing impaired and normal hearing infants. *Cerebral Cortex*, *21*(5), 991–998. https://doi.org/10.1093/cercor/bhq164

Smith, S. M., Fox, P. T., Miller, K. L., Glahn, D. C., Fox, P. M., Mackay, C. E., ... Laird, A. R. (2009). Correspondence of the brain's functional architecture during activation and rest. *Proceedings of the National Academy of Sciences of the United States of America*, *106*(31), 13040–13045.

Smyser, C. D., & Neil, J. J. (2015). Use of resting-state functional MRI to study brain development and injury in neonates. *Seminars in Perinatology*, *39*(2), 130–140.

Song, J. J., Vanneste, S., Lazard, D. S., Van de Heyning, P., Park, J. H., Oh, S. H., & De Ridder, D. (2015). The role of the salience network in processing lexical and nonlexical stimuli in cochlear implant users: An ALE meta-analysis of PET studies. *Human Brain Mapping*, *36*(5), 1982–1994. https://doi.org/10.1002/hbm.22750

Stevens, M. N., Dubno, J. R., Wallhagen, M. I., & Tucci, D. L. (2019). Communication and healthcare: Self-reports of people with hearing loss in primary care settings. *Clinical Gerontologist*, *42*(5), 485–494. https://doi.org/10.1080/07317115.2018.1453908

Stolzberg, D., Butler, B. E., & Lomber, S. G. (2018). Effects of neonatal deafness on resting-state functional network connectivity. *NeuroImage*, *165*, 69–82.

Tarabichi, O., Kozin, E. D., Kanumuri, V. V., Barber, S., Ghosh, S., Sitek, K. R., ... Lee, D. J. (2017). Diffusion tensor imaging of central auditory pathways in patients with Sensorineural hearing loss: A systematic review. *Otolaryngology and Head and Neck Surgery*, *194599817739838*, 432–442. https://doi.org/10.1177/0194599817739838

Thomason, M. E., Dassanayake, M. T., Shen, S., Katkuri, Y., Alexis, M., Anderson, A. L., ... Hassan, S. S. (2013). Cross-hemispheric functional connectivity in the human fetal brain. *Science Translational Medicine*, *5*(173), 173ra124. https://doi.org/10.1126/scitranslmed.3004978

Thomason, M. E., Dennis, E. L., Joshi, A. A., Joshi, S. H., Dinov, I. D., Chang, C., ... Gotlib, I. H. (2011). Resting-state fMRI can reliably map neural networks in children. *NeuroImage*, *55*(1), 165–175. https://doi.org/10.1016/j.neuroimage.2010.11.080

Tibbetts, K., Ead, B., Umansky, A., Coalson, R., Schlaggar, B. L., Firszt, J. B., & Lieu, J. E. (2011). Interregional brain interactions in children with unilateral hearing loss. *Otolaryngology and Head and Neck Surgery*, *144*(4), 602–611. https://doi.org/10.1177/0194599810394954

Turner, G. H., & Twieg, D. B. (2005). Study of temporal stationarity and spatial consistency of fMRI noise using independent component analysis. *IEEE Transactions on Medical Imaging*, *24*(6), 712–718.

Uddin, L. Q., Kelly, A. M. C., Biswal, B. B., Castellanos, F. X., & Milham, M. P. (2009). Functional connectivity of default mode network components: Correlation, anticorrelation, and causality. *Human Brain Mapping*, *30*(2), 625–637.

Wang, S., Chen, B., Yu, Y., Yang, H., Cui, W., Li, J., & Fan, G. G. (2019). Alterations of structural and functional connectivity in profound sensorineural hearing loss infants within an early sensitive period: A combined DTI and fMRI study. *Developmental Cognitive Neuroscience*, *38*, 100654. https://doi.org/10.1016/j.dcn.2019.100654

Wang, X., Fan, Y., Zhao, F., Wang, Z., Ge, J., Zhang, K., ... Liu, P. (2014). Altered regional and circuit resting-state activity associated with unilateral hearing loss. *PLoS One*, *9*(5), e96126. https://doi.org/10.1371/journal.pone.0096126

Wong, C., Chabot, N., Kok, M. A., & Lomber, S. G. (2014). Modified areal cartography in auditory cortex following early- and late-onset deafness. *Cerebral Cortex*, *24*(7), 1778–1792.

Xia, S., Song, T., Che, J., Li, Q., Chai, C., Zheng, M., & Shen, W. (2017). Altered brain functional activity in infants with congenital bilateral severe sensorineural hearing loss: A resting-state functional MRI study under sedation. *Neural Plasticity*, *2017*, 1–8. https://doi.org/10.1155/2017/8986362

Yang, M., Chen, H. J., Liu, B., Huang, Z. C., Feng, Y., Li, J., ... Teng, G. J. (2014). Brain structural and functional alterations in patients with unilateral hearing loss. *Hearing Research*, *316*, 37–43. https://doi.org/10.1016/j.heares.2014.07.006

Zhang, D., & Raichle, M. E. (2010). Disease and the brain's dark energy. *Nature Reviews Neurology*, *6*(1), 15–28. https://doi.org/10.1038/nrneurol.2009.198

Zhang, G. Y., Yang, M., Liu, B., Huang, Z. C., Chen, H., Zhang, P. P., ... Teng, G. J. (2015). Changes in the default mode networks of individuals with long-term unilateral sensorineural hearing loss. *Neuroscience*, *285*, 333–342. https://doi.org/10.1016/j.neuroscience.2014.11.034

Zhang, G. Y., Yang, M., Liu, B., Huang, Z. C., Li, J., Chen, J. Y., ... Teng, G. J. (2016). Changes of the directional brain networks related with brain plasticity in patients with long-term unilateral sensorineural hearing loss. *Neuroscience*, *313*, 149–161. https://doi.org/10.1016/j.neuroscience.2015.11.042

SUPPORTING INFORMATION

Additional supporting information may be found online in the Supporting Information section at the end of this article.